A Statistical Methodology of Cyclic Plasticity Inhomogeneity at Grain Scale

Zhanguang Zheng[1,2,*], Kaiming Wan[1], Tao Xu[1] and Liping Jiang[1,3]

[1]*College of Mechanical Engineering, Guangxi University, No.100 Daxue Dong Road, Nanning 530004, China*

[2]*State Key Laboratory of Featured Metal Materials and Life-cycle Safety for Composite Structures, Guangxi University, No.100 Daxue Dong Road, Nanning 530004, China*

[3]*School of Mechanical and Automotive Engineering, Guangxi University of Science and Technology, No.19 Guantang Road, Liuzhou, 545006, China*

Abstract: The inhomogeneous plastic deformation has important effects on the manufacturing process and the fatigue property of mechanical products. To directly and correctly evaluate the deformation inhomogeneity of grain scale under cyclic loading, a statistical method is proposed and named as the normalized standard deviation. The method is comprised of the following steps: (1) Construct a representative volume element (RVE) of polycrystalline by Voronoi tessellation and electron backscatter diffraction, and calculate the grain strain by a constitutive model of crystal cyclical plasticity. (2) Deal with grain strain data of RVE by Min-max normalization method. (3) Compute the standard deviation of the normalized data as the identification of mesoscopic inhomogeneity. In order to validate the proposed normalized standard deviation, the contrastive analyses with the strain contours, the weighted standard deviation and the coefficient of variation are conducted at the same conditions of cyclic loading. The results demonstrated that the normalized standard deviation was the best as the indication of cyclic plasticity inhomogeneity among the above methods.

Keywords: Strain cycle, Strain inhomogeneity, Crystal plasticity, RVE model.

1. INTRODUCTION

Polycrystalline metals are generally assumed as homogeneous in engineering applications [1], while their mechanical behaviors are very inhomogeneous at grain scale [2]. Since the shape, size and orientation of grains are different from each other [3], strain incompatibility will occur between two grains and then lead to inhomogeneous deformation [4, 5]. Because the inhomogeneous plastic deformation has important effect on micro metal forming [4, 5], surface roughness [6, 7], fatigue crack nucleation [8-10], and so on, correctly evaluating the deformation inhomogeneity at grain scale has great significance for improving the design theories and manufacturing process of products.

To the best of authors' knowledge, three methods of the strain contour [11, 12], the weighted standard deviation [13-15] and the coefficient of variation [16] have been widely used to evaluate the inhomogeneous deformation under cyclic loading. With the method of strain contour, using the picture of strain distribution [11] or extracting the grain strain along a selected line [12] is to analyze the deformation inhomogeneities of materials. This method of describing inhomogeneity is easy, but it cannot quantitatively evaluate the evolution of the whole inhomogeneities.

*Address correspondence to this author at the College of Mechanical Engineering, Guangxi University, No.100 Daxue Dong Road, Nanning 530004, China; E-mail: zhenglight@126.com

With the method of weighted standard deviation, the governing formulas take the following forms:

$$\bar{\varepsilon}_{\mathrm{ij}}=\sum_{k=1}^{nSRVE}\left(\varepsilon_{\mathrm{ij}}\right)_k p_k \quad , \quad \hat{\varepsilon}_{\mathrm{ij}}=\sqrt{\sum_{k=1}^{nSRVE}\left(\varepsilon_{\mathrm{ij}}\right)_{\mathrm{k}}^2 p_k-\bar{\varepsilon}_{ij}^2} \quad , \quad \mathrm{p}_k=\frac{\Delta V_k}{V} \tag{1}$$

where nSRVE is the total number of the finite elements contained in the SRVE; is the mean strains of the SRVE; is, respectively, the strains of the k-th element; denotes the volume of the k-th element, and *V* is the total volume of the SRVE.

The method of weighted standard deviation can quantitatively evaluate the inhomogeneity at every time of cyclic deformation and is applied to predict the low-cycle fatigue life of metals [13, 14]. However, the above inhomogeneity at every time cannot be compared with each other. It is because the applied loading to calculate the grain strain is different at every time and the resulting mean strain of grains is also different. This is said that the standard deviation cannot be applied directly to compare the variation of the mark for the general population of different levels [15].

With the method of variation coefficient [16], the governing formulas take the following forms:

$$\mathrm{s}=\frac{\hat{\sigma}_{\mathrm{ij}}}{\bar{\sigma}_{\mathrm{ij}}} \quad , \quad \hat{\sigma}_{\mathrm{ij}}=\sqrt{\frac{1}{\mathrm{n}}\sum_{k=1}^{n}\left[\left(\sigma_{\mathrm{ij}}\right)_{\mathrm{k}}-\bar{\sigma}_{\mathrm{ij}}\right]^2} \quad , \quad \bar{\sigma}_{\mathrm{ij}}=\frac{\sum_{k=1}^{n}\left(\sigma_{\mathrm{ij}}\right)_k}{\mathrm{n}} \tag{2}$$

where n is the total number of the finite elements

Received on 03-06-2025 Accepted on 11-07-2025 Published on 15-07-2025

E-ISSN: 2409-9848/25

contained in the SRVE; is the standard deviation of stress of the SRVE. is the mean stress of the SRVE; is, respectively, the stress of the k-th element.

The method of variation coefficient can quantitatively describe the inhomogeneous deformation of the material, and can be used to compare the inhomogeneity of the material at any time of cyclic deforming. However, once the mean strain as the denominator is small, the ratio of the standard deviation to the mean strain will increase abnormally and lead to the results inaccurate.

To solve the problems of the above three methods, a normalized standard deviation is proposes to describe the inhomogeneity of material deformation. Firstly, the finite element analysis of crystal plasticity for the cyclic behavior of polycrystals in the RVE; Secondly, the Min-max normalization method for cyclic plasticity data preprocessing, Lastly, calculate the standard deviation of the preprocessed data to quantitatively describe the heterogeneous of metal deformation.

2. DESCRIPTION OF INHOMOGENEITY BASED ON CRYSTAL PLASTICITY

2.1. Constitutive Models

The crystal plasticity model is formulated by Asaro and Needleman (1985) and used by Inal *et al* [17]. A total deformation gradient is given as follows [18]:

$$F = F^e \cdot F^p \tag{3}$$

Where F^e refers to the deformation gradient produced by lattice distortion and rigid rotation, F^p represents the deformation gradient corresponding to the uniform shear of the crystal along the slip direction.

The above equation allows the velocity gradient to be divided into two parts.

$$L = L^e + L^p \tag{4}$$

L^e is the corresponding lattice distortion and rigid rotation part. L^p is the corresponding slip part, among them

$$L^P = \sum_{\alpha=1}^{N} \dot{\gamma}^\alpha m^\alpha \otimes n^\alpha \tag{5}$$

$\dot{\gamma}^\alpha$ denotes the shear strain rate on the α slip system. m^α and n^α are the direction vector and the normal vector of the α slip system respectively. The plastic part of the velocity gradient can be decomposed into a symmetrical part D^P and an anti-symmetric part W^P, given by the following formulas:

$$D^P = \frac{1}{2}(L^P + L^{P^T}) = \sum_{\alpha=1}^{N} \frac{1}{2}(m^\alpha \otimes n^\alpha + n^\alpha \otimes m^\alpha)\dot{\gamma}^\alpha = \sum_{\alpha=1}^{N} P^\alpha \dot{\gamma}^\alpha \tag{6}$$

$$W^P = \frac{1}{2}(L^P - L^{P^T}) = \sum_{\alpha=1}^{N} \frac{1}{2}(m^\alpha \otimes n^\alpha - n^\alpha \otimes m^\alpha)\dot{\gamma}^\alpha = \sum_{\alpha=1}^{N} W^\alpha \dot{\gamma}^\alpha \tag{7}$$

The microscopic deformation in polycrystalline materials follows the deformation law of the single crystal. Hill, Rice, Asaro and Hutchinson have established and developed a plasticity theory for describing plastic deformation of the crystal. The elastic deformation is determined by the anisotropic elastic stress-strain relationship. The plastic deformation part is determined by the relationship between shear rate and shear stress of all activated slip systems. For a rate-dependent inelastic formula, which the plastic slip rate for a given slip system follows a power law given by [19]:

$$\dot{\gamma}^\alpha = \dot{\gamma}_0 \left| \frac{\tau^\alpha - x^\alpha}{g^\alpha} \right|^m \operatorname{sgn}(\tau^\alpha - x^\alpha) \tag{8}$$

Where $\dot{\gamma}^\alpha$ denotes the reference strain rate; τ^α is the resolved shear stress on the α-slip system and x^α is backstress; m is the rate sensitivity coefficient; g^α is the plastic slip hardening function of the α slip system according to:

$$\dot{g}^\alpha = \sum_{\beta=1}^{N} h_{\alpha\beta}(\gamma) \left| \dot{\gamma}^\beta \right| \tag{9}$$

where $h_{\alpha\beta}(\gamma)$ are the slip-plane hardening moduli, which is given by:

$$h_{\alpha\beta}(\gamma) = qh(\gamma) + (1 - q)\,\delta_{\alpha\beta} h(\gamma) \tag{10}$$

where the self hardening modulus $h(\gamma)$ is obtained as:

$$h(\gamma) = h_0 \operatorname{sech}^2\left(\frac{h_0 \gamma}{\tau_s - \tau_0}\right) \tag{11}$$

Where h_0 is the initial hardening modulus ; τ_0 is the initial critical resolved shear stress; τ_s is the saturation value of critical resolved shear stress and γ is the accumulated shear strain in all slip systems, which is expressed as:

$$\gamma = \int \sum_{\alpha}^{n} \left| d\gamma(\alpha) \right| \tag{12}$$

The kinematic hardening x^α [20] is:

$$\dot{\chi}^{\alpha} = a\dot{\gamma}^{\alpha} - c\left[1 - e_1\left(1 - \exp\left(-e_2\gamma\right)\right)\right]\chi^{\alpha}\left|\dot{\gamma}^{\alpha}\right| - p\chi^{\alpha} \quad (13)$$

where a is the material constant representing linear hardening; c and p are the material constants representing nonlinear hardening; e_1 and e_2 are the material constants that regulates the saturation value of nonlinear hardening.

2.2. A Method of Mesoscopic Strain Inhomogeneity Description

Considering the above limits of the strain contours, the weighted standard deviation and the coefficient of variation, a statistical method is proposed to describe the deformation inhomogeneity at grain scale, and the method is named as the normalized standard deviation. The calculation steps of this method are as follows: (1) Min-max normalization method is adopted; (2) The standard deviation of the normalized data is computed as the identification of mesoscopic strain inhomogeneity.

Firstly, the crystal grain interior stresses and plastic strains are calculated on the basis of the crystal plasticity model and the user-supplied subroutine UMAT implemented in the FE code ABAQUS.

Secondly, Min-max normalization method is adopted to preprocess the plastic strain of every element in the RVE under cyclic loading, and the normalization equation can be described as the following formula [21]:

$$\left(\varepsilon_{ij}^{*}\right)_k = \frac{\left(\varepsilon_{ij}\right)_k - \varepsilon_{\min}}{\varepsilon_{\max} - \varepsilon_{\min}} \quad (14)$$

where ε_{ij}^{*} and ε_{ij} are the normalized strain value and the longarithmic strain tensor, respectively; the subscript contained *k* denotes the k-th element in the RVE; $\varepsilon_{\min}$ is the minimum longarithmic strain and $\varepsilon_{\max}$ is the maximum longarithmic strain of all elements. By the min-max data normalization method, the strains of all elements become the dimensionless data in the range of [0, 1].

Lastly, to describe meso-strain inhomogeneity of the above elements, the statistical analyses are implemented to obtain the mean value and the standard deviation of the preprocessed data. The governing formulas take the form:

$$\hat{\varepsilon}_{ij} = \sqrt{\frac{1}{n}\sum_{k=1}^{n}\left[\left(\varepsilon_{ij}^{*}\right)_k - \overline{\varepsilon_{ij}^{*}}\right]^2}, \quad \overline{\varepsilon_{ij}^{*}} = \frac{\sum_{k=1}^{n}\left(\varepsilon_{ij}^{*}\right)_k}{n} \quad (15)$$

Where n is the total number of finite elements in the RVE; $\overline{\varepsilon_{ij}^{*}}$ is the mean value of all normalized strains; $\hat{\varepsilon}_{ij}$ is the corresponding standard deviation of ε_{ij}^{*} in the RVE.

3. VALIDATION

3.1. Materials and Experiments

The used material is ultrafine grained pure copper (T2), which is processed by equal-channel angular pressing. After 8 passes of equal-channel angular pressing, microstructures of the specimens are investigated by Electron Backscatter Diffraction (EBSD). The inverse pole figures and grain size distributions of ultrafine grained pure copper are shown in Figure **1**. As shown in Figure **1**(**b**), the average grain diameter is about 1 μm.

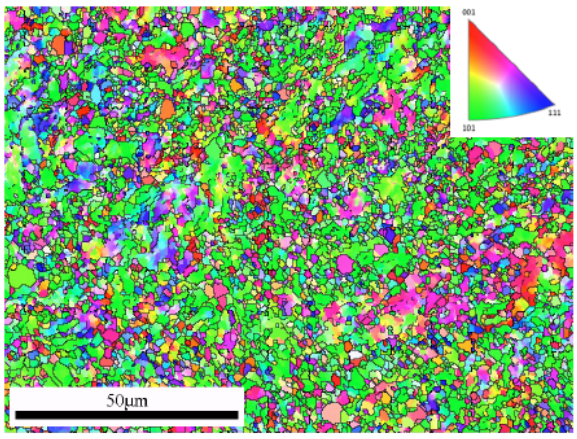

(**a**)The grain morphology of the ultrafine-grain pure copper

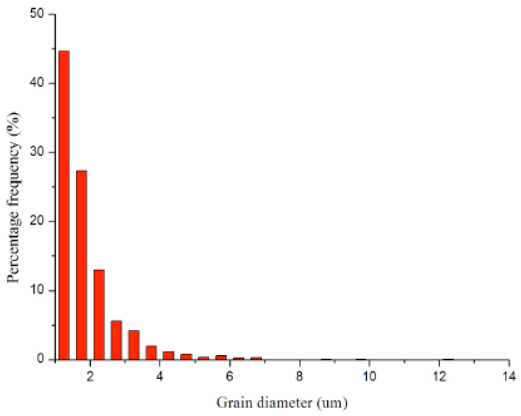

(**b**) The distribution histogram of grain size

Figure 1: The EBSD map of the ultrafine-grain pure copper.

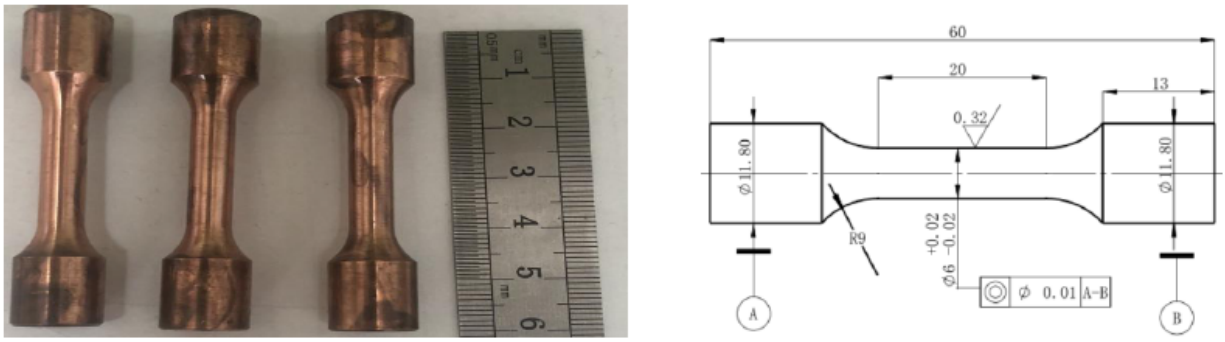

Figure 2: The specimens of uniaxial tensile and symmetrical cyclic tensile-compressive experiments.

To identify the parameters of constitutive model based on crystal cyclic plasticity, some uniaxial tensile and symmetrical tensile-compressive cyclic loading experiments are conducted using a servo-hydraulic load frame which has a capacity of±20kN in the axial load. The testing system was controlled by a computer, and the specimens are shown as Figure **2**. For the monotonic loading experiments and the strain-controlled cyclic loading experiments, a clip-on extensometer with a gage length of 12.5 mm and a range of ±10% was used for the strain measurement. All the experiments were conducted in ambient air.

3.2. Parameter Identification and Validation of the Constitutive Model

3.2.1. Voronoi Tessellation and Boundary Conditions

The representative volume element (RVE) is used to reflect the configuration and size of grain and lattice orientation of metal materials. The RVE model is constructed by Voronoi tessellation as displayed in Figure **2** [14]. The details are as follows: (1) The RVE consists of 20 × 20 × 20= 8,000 C3D8R elements and 9,261 nodes. (2) The coordinates of grain's crystal nucleus of all the 100 grains are generated by random numbers, and then the 8000 units are divided into 100 grains. The initial crystal orientations of each grain are implemented from EBSD to RVE by python software.

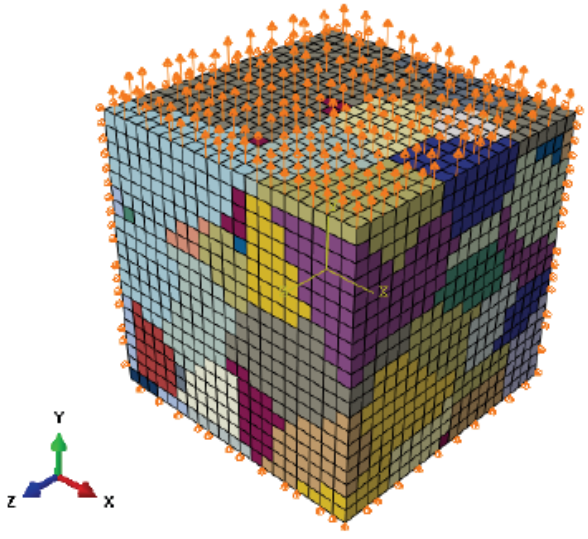

Figure 3: The boundary conditions of RVE.

The boundary conditions are shown in Figure **3**: The bottom plane (x-z) of the RVE is constrained by U2=0, the left rear plane (y-z) by U1=0, and the right rear plane (x-y) by U3=0, respectively. Then a displacement in the y direction is applied on the top plane, where the magnitude of the displacement is coincided with the experiment.

3.2.2. Parameter Identification of the Constitutive Model

According to the above experimental conditions, the stress-strain curves of uniaxial tensile and the stable hysteresis loops under different strain amplitudes (0.4%, 0.5%, 0.6% and 0.8 %) are obtained. Then the RVE model of 100 grains is fitted by simulating uniaxial tensile stress-strain curve (Figure **4**) and hysteretic curve (Figure **5**) with reference to the experimental data, respectively. The model parameters are determined as shown in Table **1**.

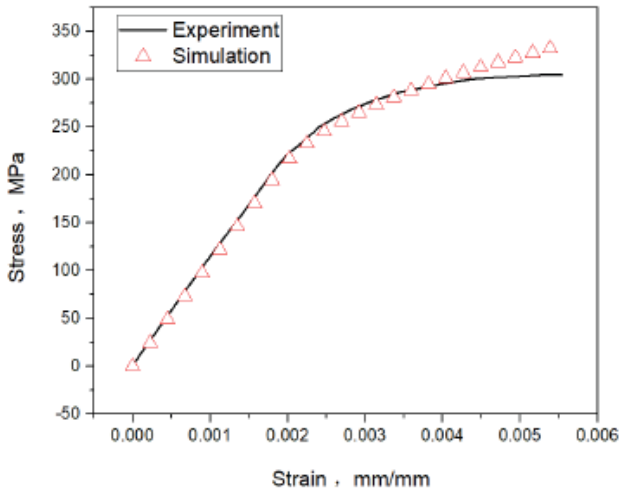

Figure 4: The comparison of experiments and simulations, the stress–strain curves of ultrafine copper under the uniaxial tensile.

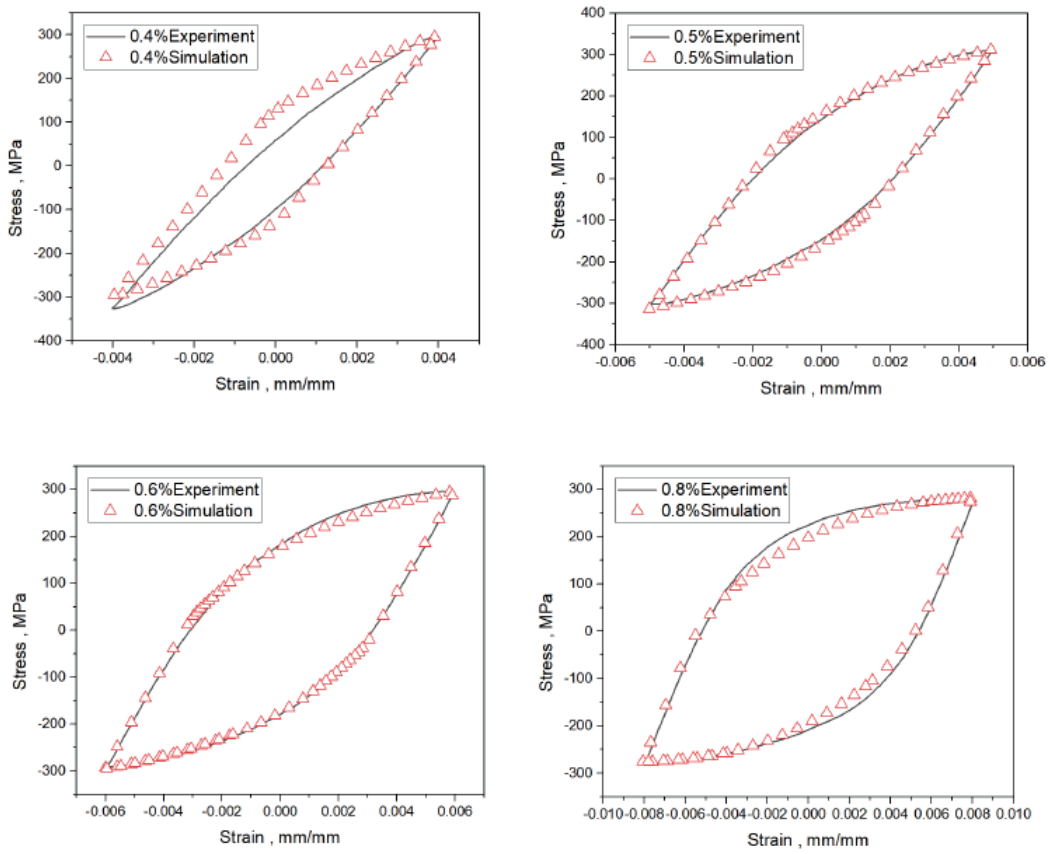

Figure 5: The comparison of experimental results and simulations, stable stress–strain hysteresis loops under uniaxial cyclic deformation with R = −1 with strain amplitudes of 0.4%, 0.5%, 0.6% and 0.8%.

Table 1: Material parameters of ultrafine pure copper constitutive model

C11 /GPa	C12 /GPa	C44 /GPa	τ_s /MPa	τ_0 /MPa	h0 /MPa	m	a /GPa	c /GPa	e1	e2	p	$\dot{\gamma}_0$ /s-1
141346	60577	40385	50	100	-80	80	20	0.2	-0.5	2	0	0.001

3.3. Case Analysis and Comparison Among Four Methods

Because the stable hysteresis loops under the strain amplitude of 0.8 % is the most representative in Figure **5**, the symmetrical tensile-compressive cyclical experiments under strain amplitude of 0.8 % are selected as the case analysis of all above methods. For the statistical analyzability of the computed data, the second cycle and the third cycle with strain amplitude of 0.008 are taken as an example to evaluate the strain inhomogeneity. According to statistics, standard deviation can be directly used to compare the dispersion of fluctuant data only with the same mean values. Therefore, the displacements of ±0.005 moment are taken as the examples. The strain inhomogeneity from point A to point H is obtained and analyze by the four methods, which can describe the inhomogeneous deformation during cyclic loading of materials as follows.

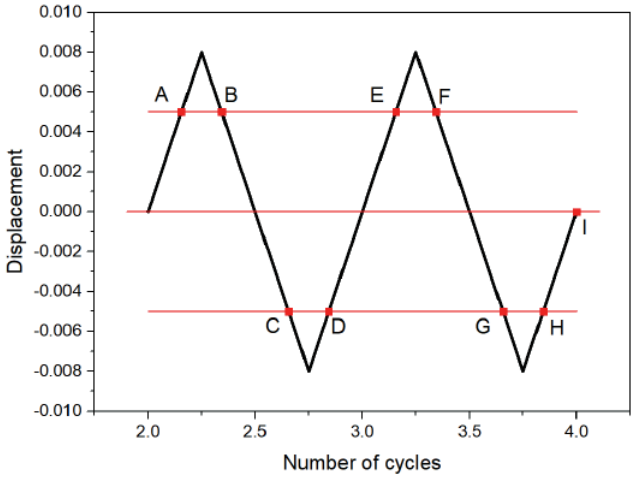

Figure 6: The variation of the displacement in the second cycle and the third cycle with strain amplitude of 0.008; the displacement of ±0.005 is expressed as eight points from A to H during the cycling; the displacement of 0 at the end of the third cycle is expressed as I.

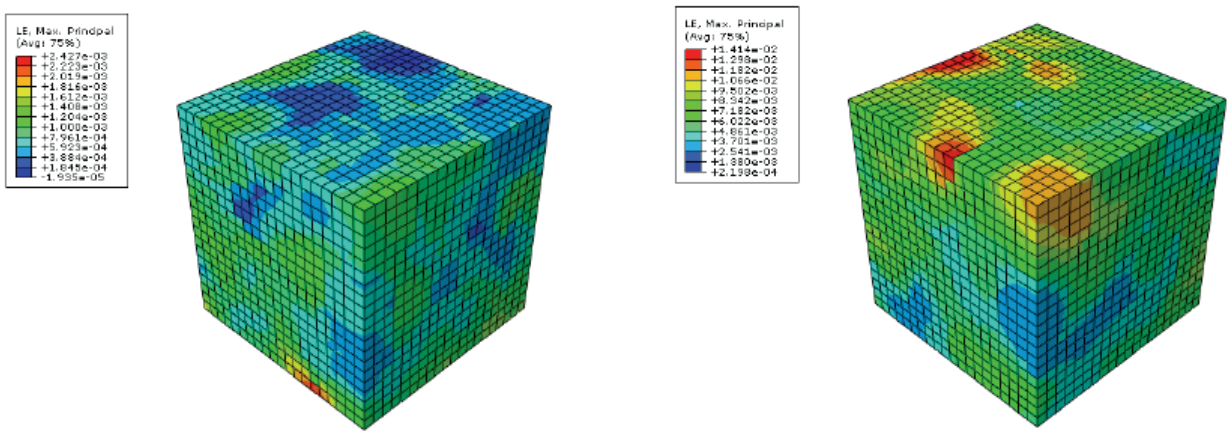

(**a**) The true strain distribution of point A

(**b**) The true strain distribution of point E

Figure 7: The true strain distribution of point A and E in Figure **6**.

The strain contours method is used to assessment the inhomogeneity of strain distributions by taking the point A and point E in Figure **6** as an example, the pictures which describe the true strain situation of the two points are shown in Figures **7**(**a**) and (**b**). It can be seen that the true strain distribution of the RVE is changing during the cycling. We can only roughly compare the inhomogeneities of RVE surface, but it is difficult to express the interior strain, and to accurately quantify the variation of the RVE strain during the entire process.

The remaining three methods can quantitatively describe the inhomogeneity of the RVE strain. The differences among the calculated data of the three methods are too large to be directly compared, so the three sets of data are linearly transformed to the value range between 0 and 1 as shown in Figure **8**.

It can be seen from Figure **8** that the strain inhomogeneities at the displacement of ±0.005 in different cycles are in the evolution. The overall trend of the inhomogeneities calculated by the strain between the normalized and the weighted standard deviation methods are similar except only point C and point G, but the coefficient of variation method is different from the above trend. For example, the values of points D and H calculated by the standard deviation method and the normalized standard deviation method are respectively higher than that of the points C and G, while the coefficient of variation method is on the contrary. Although Figure **8** provides a preliminary comparison of the predictability of the three methods, it still does not confirm which method is the best. In order to accurately judge the usability of the three methods, the compared analyses of the four irregular points C, D,

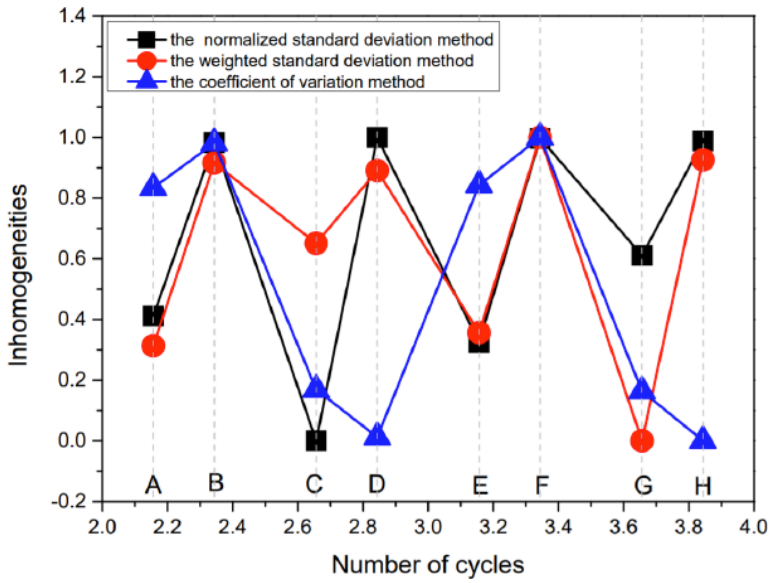

Figure 8: Three methods for describing strain inhomogeneity during cyclic stretching with the amplitudes of 0.005 in the 3rd cycle and 4th cycle; the eight points from A to H have the same meaning as in Figure **6**.

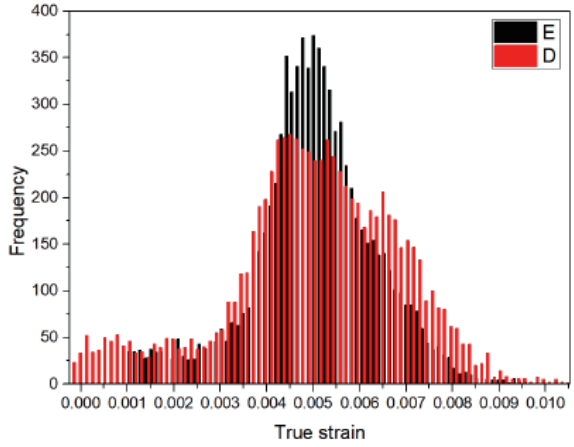

(**a**) Compare point D and point E in Figure **8**

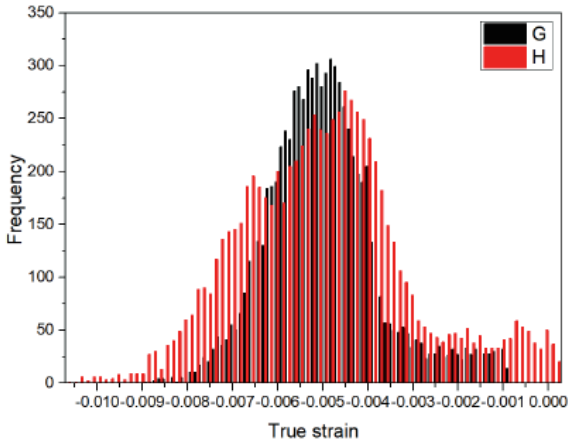

(**b**) Compare point G and point H in Figure **8**

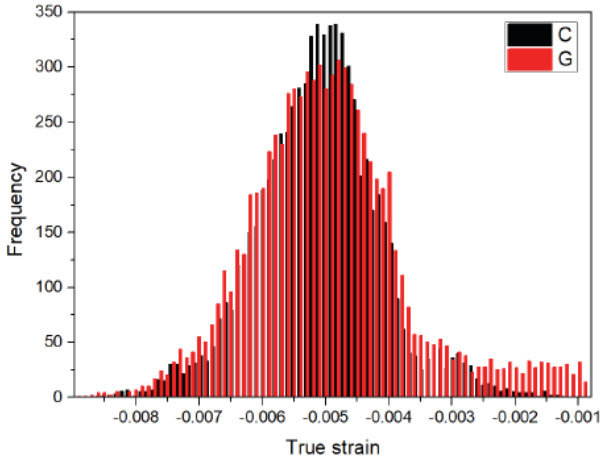

(**c**) Compare point C and point G in Figure **8**

Figure 9: True strain-frequency distribution diagram at different points.

G and H with the other regular points are carried out by strain-frequency distribution diagram.

At first, the strain-frequency distribution diagrams of all elements at points D and E of Figure **8** are showed in Figure **9**(**a**). The variation range of the element strains at point D is larger than that at point E, and the peak value of point D is smaller than that of point E. Therefore, the deformation inhomogeneity of point D is greater than that of point E. Similarly, point H should also be higher than point G through the analyses of the strain-frequency distribution diagrams in Figure **9**(**b**). However, in Figure **7**, the deformation inhomogeneities of points D and H are smaller than those of points E and G calculated by the coefficient of variation method, respectively. These are demonstrated that the coefficient of variation method is not accurate in describing the deformation inhomogeneity.

Then, the strain-frequency distribution diagrams of all elements at points C and G of Figure **8** are showed in Figure **9**(**c**). The variation range of the element strains at point G is larger than that at point C, and the peak value is smaller than that at point C. Therefore, the deformation inhomogeneity of point G is larger than that of point C. In Figure **8**, the deformation inhomogeneity of point G are larger than that of point C calculated by the normalized standard deviation method, but the result of the weighted standard deviation method is contrary. It is demonstrated that the normalized standard deviation method is more accurate than the weighted standard deviation method in describing the deformation inhomogeneity.

4. CONCLUSIONS

(1) Ultrafine grained pure copper (T2) with grain size about 1 μm is taken as experimental materials to identify the constitutive model parameters of crystal plasticity under uniaxial tensile of quasi-static state and symmetric strain cycle loading of different strain amplitudes (0.4%, 0.5%, 0.6% and 0.8 %).

(2) On the basis of the RVE consisting of a polycrystalline aggregation and the crystal plasticity theory, the simulations can capture the experimental stress-strain hysteresis loops and represent the inhomogeneous microstructures evolutions of materials.

(3) A statistical method of mesoscopic inhomogeneity description is proposed, which is named as the normalized standard deviation. The method is comprised of the following two steps: (1) Min-max normalization method is adopted to deal with the strain of every grain in RVE; (2) The standard deviation of the normalized data is computed as the identification of mesoscopic inhomogeneity.

(4) By the contrasts of four methods at the same conditions, the proposed normalized standard deviation has overcome the limits of the strain contours, the weighted standard deviation and the coefficient of variation, and can be applied to directly and correctly evaluate the deformation inhomogeneity of grain scale under cyclic loading.

DECLARATION OF COMPETING INTEREST

The authors declare that they have no known competing financial interests or personal relationships that could have appeared to influence the work reported in this paper.

ACKNOWLEDGMENTS

This research was sponsored by the National Natural Science Foundation of China (52265018 and 51675110), the Natural Science Foundation of Guangxi (2025GXNSFDA069015) and Innovation Project of Guangxi Graduate Education (YCBZ2025053).

REFERENCES

[1] Furushima T, Nakayama T, Sasaki K. A new theoretical model of material inhomogeneity for prediction of surface roughening in micro metal forming. CIRP Annals 2019; 68(1): 257-260. https://doi.org/10.1016/j.cirp.2019.04.057

[2] Zhang MH, Shen XH, He L, *et al*. Investigation of deformation inhomogeneity and low-cycle fatigue of a polycrystalline material. Appl Sci-Basel 2021; 11(6): 2673. https://doi.org/10.3390/app11062673

[3] Zheng ZG, Xie CJ, Chen JX, *et al*. A crystal plasticity model of low cycle fatigue damage considering dislocation density, stress triaxiality and Lode parameter. Int J Fatigue 2023; 175: 107823. https://doi.org/10.1016/j.ijfatigue.2023.107823

[4] Wouters O, Vellinga WP, Tijum R, *et al*. Effects of crystal structure and grain orientation on the roughness of deformed polycrystalline metals. Acta Mater 2006; 54(10): 2813-2821. https://doi.org/10.1016/j.actamat.2006.02.023

[5] Raabe D, Sachtleber M, Weiland H, *et al*. Grain-scale micromechanics of polycrystal surfaces during plastic straining. Acta Mater 2003; 51(6): 1539-1560. https://doi.org/10.1016/S1359-6454(02)00557-8

[6] Bong HJ, Lee J. Crystal plasticity finite element-Marciniak-Kuczynski approach with surface roughening effect in predicting formability of ultra-thin ferritic stainless steel sheets. Int J Mech Sci 2021; 191: 106066. https://doi.org/10.1016/j.ijmecsci.2020.106066

[7] Liu, CS, Xu WJ, Liu MY, *et al*. Effect of strain path on roughness evolution of free surface during plastic deformation. Int J Mech Sci 2020; 173: 105475. https://doi.org/10.1016/j.ijmecsci.2020.105475

[8] Ghosh S, Chakraborty P. Microstructure and load sensitive fatigue crack nucleation in Ti-6242 using accelerated crystal plasticity FEM simulations. Int J Fatigue 2013; 48: 231-246. https://doi.org/10.1016/j.ijfatigue.2012.10.022

[9] Guo N, Sun K, Tang B, *et al*. In-situ deformation inhomogeneity and damage evolution of mixed-grain structure with tempered sorbite/bainite in Fe-Cr-Mo-Mn steel. Mat Sci Eng A-struct 2024; 903: 146684. https://doi.org/10.1016/j.msea.2024.146684

[10] Wang H, Yang P, Xie Q, *et al*. Crystal plasticity finite element study on orientation evolution and deformation inhomogeneity of island grain during the ultra-thin strips rolling of grain oriented electrical steel. Materials 2024; 17(24): 6276. https://doi.org/10.3390/ma17246276

[11] Zhao J, Lv LX, Liu G, *et al*. Analysis of deformation inhomogeneity and slip mode of TA15 titanium alloy sheets during the hot tensile process based on crystal plasticity model. Mat Sci Eng A-struct 2017; 707: 30-39. https://doi.org/10.1016/j.msea.2017.08.094

[12] Li M, Barrett RA, Scully S, *et al*. Cyclic plasticity of welded P91 material for simple and complex power plant connections. Int J Fatigue 2016; 87: 391-404. https://doi.org/10.1016/j.ijfatigue.2016.02.005

[13] Liu GY, Zhang KS, Zhong XC, *et al*. Analysis of meso-inhomogeneous deformation on a metal material surface under low-cycle fatigue. Acta Mech Solida Sin 2017; 30(6): 557-572. https://doi.org/10.1016/j.camss.2017.11.002

[14] Zhang KS, Shi YK, Ju JW. Grain-level statistical plasticity analysis on strain cycle fatigue of a FCC metal. Mech Mater 2013; 64: 76-90. https://doi.org/10.1016/j.mechmat.2013.05.001

[15] Zhang KS, Ju JW, Li ZH, *et al*. Micromechanics based fatigue life prediction of a polycrystalline metal applying crystal plasticity. Mech Mater 2015; 85: 16-37. https://doi.org/10.1016/j.mechmat.2015.01.020

[16] Xu L, Qiao G, Ma Y, *et al*. Numerical study of deformation inhomogeneity and its effect on mechanical properties of the heavy-wall offshore pipeline fabricated by different processes. Ocean Eng 2025; 323: 120656. https://doi.org/10.1016/j.oceaneng.2025.120656

[17] Li F, Liu C, Cao Y, *et al*. Deformation inhomogeneity evolution and crack formation mechanism analysis in ultra-high strength steel by crystal plasticity simulations. Eng Fail Anal 2024; 163: 108502. https://doi.org/10.1016/j.engfailanal.2024.108502

[18] Sun T, Qin LD, Xie YJ, *et al*. An approach for predicting the low-cycle-fatigue crack initiation life of ultrafine-grained aluminum alloy considering inhomogeneous deformation and microscale multiaxial strain. Materials 2022; 15(9): 3403. https://doi.org/10.3390/ma15093403

[19] Feng L, Zhang G, Zhang KS. Discussion of cyclic plasticity and viscoplasticity of single crystal nickel-based superalloy in large strain analysis: comparison of anisotropic macroscopic model and crystallographic model. Inter J Mech Sci 2004; 46(8): 1157-1171. https://doi.org/10.1016/j.ijmecsci.2004.08.003

[20] Zhang KS, Shi YK, Xu LB. Anisotropy of yielding/hardening and micro inhomogeneity of deforming/rotating for a polycrystalline metal under cyclic tension-compression. Acta Metall Sin 2011; 47(10): 1292-1300.

[21] Wen H, Pan S, Gao W, *et al*. Real-time single-frequency GPS/BDS code multipath mitigation method based on C/N0 normalization. Measurement 2020; 164: 108075. https://doi.org/10.1016/j.measurement.2020.108075

https://doi.org/10.31875/2409-9848.2025.12.04

© 2025 Zheng *et al*.
This is an open-access article licensed under the terms of the Creative Commons Attribution License (http://creativecommons.org/licenses/by/4.0/), which permits unrestricted use, distribution, and reproduction in any medium, provided the work is properly cited.